

# Ultraviolet Spectra of ULX Systems

Joel N. Bregman, Julie N. Felberg, Patrick J. Seitzer

*Department of Astronomy, University of Michigan, Ann Arbor, MI 48109*

`jbreman@umich.edu`

Jifeng Liu

*Eureka Scientific, Oakland, CA 94602*

and

Martin Kümmel

*Space Telescope Science Institute, Baltimore, MD 21218*

## ABSTRACT

To further understand the nature of the optical counterparts associated with Ultraluminous X-Ray sources (ULXs), we obtained far ultraviolet spectra of the reported counterparts to the ULXs in NGC 1313, Holmberg II, NGC 5204, and M81. The spectral resolution of the ACS prism spectra degrades from 300 at 1300Å to 40 at 1850Å so longer wavelength features have lower S/N. The spectra of the ULXs in NGC 1313, Ho II, and NGC 5204 are quite similar, showing the N V  $\lambda$ 1240 line at about the same equivalent width strength. The presence of this and other emission lines confirms the presence of an accretion disk, probably diluted by the light of an early B star companion. The spectra differ strongly from high mass X-ray binaries dominated by O star winds (e.g., Cyg X-1) and are most similar to intermediate mass X-ray binary systems in the Milky Way and LMC. This indicates that the mass transfer is due to Roche Lobe overflow. The spectrum of the ULX in M81 is quite weak but suggestive of a late-type Wolf-Rayet star.

*Subject headings:* X-rays: binaries

## 1. Introduction

Ultraluminous X-ray sources (ULXs) are a class of X-ray point sources, mostly in the disks of spiral galaxies, with X-ray luminosities exceeding the Eddington luminosity ( $L_{Ed}$ ) of the most massive known stellar mass black holes in the Milky Way, Cygnus X-1 ( $16 M_{\odot}$  and  $L_{Ed} = 2 \times 10^{39} \text{ erg s}^{-1}$ ; Fabbiano 2006). There is typically one ULX per spiral galaxy with luminosities sometimes exceeding  $10^{40} \text{ erg s}^{-1}$  (e.g., Liu & Bregman 2012). A few explanations are generally offered to explain ULXs, all involving mass transfer from a donor star to a black hole. These ULXs could be intermediate mass black holes ( $10^2$ - $10^4 M_{\odot}$ ) that are emitting at 0.01-0.1 of  $L_{Ed}$ , similar in efficiency to their lower-mass counterparts (Colbert and Mushotzky 1999). Another explanation is that they are exceeding  $L_{Ed}$  due to the accretion disk somehow accommodating this higher luminosity through exotic non-axisymmetric processes, such as photon bubbles (Begelman 2002). A third possibility is that the emission is highly anisotropic (King et al. 2001).

Not only is there uncertainty regarding the mass of the primary, there are several important unresolved issues regarding the nature of these binary systems, which, if resolved, could help appreciate the underlying physical situation. One of the issues is the nature of the secondary that is providing the mass transfer. It was expected that the secondary would be massive, as ULXs are young phenomena, primarily lying in star-forming regions that are typically 10 Myr or less. They are not in extremely dense star clusters, so dynamical interactions with other stars is unlikely in the lifetime of the ULX (we can treat them as isolated binaries). We anticipated that the secondary would have begun evolving away from the main sequence, so it would have the magnitude of an O star, but it could have any color as it expands to fill its Roche Lobe. However, when optical counterparts were discovered (mainly with HST), they were found to be blue, even after correcting for possible contamination by an accretion disk (e.g., Liu et al. 2002). This leads to the conjecture that the mass transfer is related to massive stellar winds from hot stars.

This conjecture can be tested with ultraviolet spectra of these systems, as hot stars can have distinctive far ultraviolet features. Such a program will address two issues, the first being the identification of a particular stellar object with the ULX. Many optical identifications depend on the proximity of an optical object within the error circle of an X-ray identification. Some of these identifications may occur by chance because ULXs occur in moderately crowded fields. Real and false identifications can be distinguished by UV spectra, as X-ray binaries have distinctive emission lines. The other goal is to constrain the spectral type and properties of the secondary and of the accretion disk. This is easier to accomplish in the far UV because most hot stars depart from the Rayleigh-Jeans limit (evident in the optical region) and the strongest absorption lines are from high excitation ions, which occur in the

UV region.

We study the far UV prism spectra, obtained with the Advanced Camera for Surveys on HST, for four ULXs in this paper. We first describe the target selection and data processing in §2, the analysis of the spectra in §3, then the interpretation of these spectra in the context of spectra of known objects and a color-color diagram in §4, followed by a discussion in §5.

## 2. Target Selection and Observations

From the combination of Chandra and HST imaging, a number of optical counterparts had been identified at the time this program began. In order to obtain spectra of these counterparts with a moderate number of orbits, they had to be sufficiently bright in the ultraviolet region, which required that the targets be nearby ( $D < 10$  Mpc), with moderately low dust extinction, and sufficiently high optical flux. Another consideration was crowding, as ULX optical counterparts can occur in complex regions. With the narrow slit of the STIS instrument, most confusion problems could be avoided, but when STIS suffered a failure, the only viable UV spectrograph was the prism on the Advanced Camera for Surveys. However, as there are no slits on this instrument, it could only be used for ULX fields in which source confusion could be avoided. After considering possible candidates and a variety of roll angles, we found it was possible to obtain UV spectra of four ULX optical counterparts in the galaxies Ho II, M81, NGC 1313, and NGC 5204 (Table 1). The data were obtained in Cycle 15.

For the observations, we used the Solar Blind Camera (SBC), in conjunction with the PR130L prism, which covers the wavelength range 1230Å to 1850Å; the observations comprised most of two orbits per object. A short complementary image was also obtained with the SBC, with the F165L filter, which allows one to register the spectra with the point sources and to calibrate the wavelength range. To extract the spectra, we used the aXe software package (Kümmel et al. 2009), following standard procedures. The highest quality spectra were for the ULX optical counterparts in NGC 1313 and Ho II, followed by NGC 5204, and with M81 having the poorest spectrum due to its lower flux level.

## 3. Analysis and Modeling of the Data

For spectra obtained with dispersion gratings, there is only a modest variation in the spectral resolution, while for prism spectra, the resolution can vary by a factor of several, as is the case here. Over the effective waveband of the prism spectrum, 1220–1850Å, the

resolution decreases from about 300 at  $1300\text{\AA}$  ( $1000\text{ km s}^{-1}$ ) to about 100 at  $1500\text{\AA}$  ( $3000\text{ km s}^{-1}$ ), to 40 at  $1850\text{\AA}$  ( $7500\text{ km s}^{-1}$ ). Consequently, it is easier to detect lines and their shapes at the short wavelength end, as we see in Figure 1.

We sought to identify known UV lines in these ULX systems. These systems have several components, including an accretion disk and a hot stellar companion, and where the spectrum is modified by Galactic absorption. The lines anticipated from each component can be identified, making a decomposition possible.

Galactic absorption lines: the strongest that would be detected in this wavelength region are Si II  $\lambda 1260.4$ , O I  $\lambda 1302.2$ , and C II  $\lambda 1334.5$ . These lines are completely unresolved, so they provide a local measurement of the line width.

Accretion Disks in X-Ray Binaries: Emission lines that are commonly found in X-ray binaries with accretion disks include the following high ionization lines: NV  $\lambda 1238.8$ ,  $1242.8$ , Si IV  $\lambda 1393.8$ ,  $1402.8$ , C IV  $\lambda 1548.2$ ,  $1550.8$ , and He II  $\lambda 1640.4$ .

OB Stars: Photospheric absorption lines that we searched for are Si II  $\lambda 1264.7$ , Si III  $\lambda 1298.9$ , O IV  $\lambda 1338.6$ , and Si III  $\lambda 1417.2$  (Prinja 1990). These lines are not resonance lines, so the lower level is populated through frequent collisions, which occur in the atmosphere of the star. There are other stronger lines in this wavelength range (e.g., He II), but they cannot be detected with the resolution of these prism data. P–Cygni emission lines are sometimes seen in OB stars due to their winds, primarily in the doublets of C IV  $\lambda 1548.2$ ,  $1550.8$ , and Si IV  $\lambda 1393.8$  (usually weaker).

Wolf-Rayet Stars: These stars have winds with high rates of mass loss and emission lines. The strongest emission line is often He II  $\lambda 1640.4$ , but the other prominent lines depend on whether the star has a relative excess of nitrogen or carbon, being the WN and WC designations (Niedzielski and Rochowicz 1994). For the WN stars, the N IV  $\lambda 1486.5$  line can be prominent and it is distinctive in that it is associated with high-density winds and is not predicted to be produced in accretion disks. The C IV  $\lambda 1548.2$ ,  $1550.8$  doublet is often detected in WN stars, with a P–Cygni profile, although in the WC stars, this is usually the strongest line, followed by the He II line. There is a wide range in the UV spectrum of WR stars, from having very prominent emission lines to rather weak emission.

Our inspection of the four targets led to the identification of the following features. The results are given in order of decreasing continuum flux, and therefore decreasing S/N.

Holmberg II: All three Galactic absorption features are detected. In emission, we detect the N V 1240 doublet and the He II 1640 line, and probably the Si IV doublet as well. Other features are not statistically significant, such as the N IV 1486 line or the C IV 1550 doublet. There is a hint of stellar absorption features, which would need confirmation with higher resolution spectra. The stellar Si II  $\lambda 1264.7$  line lies just to the red of the Galactic Si II

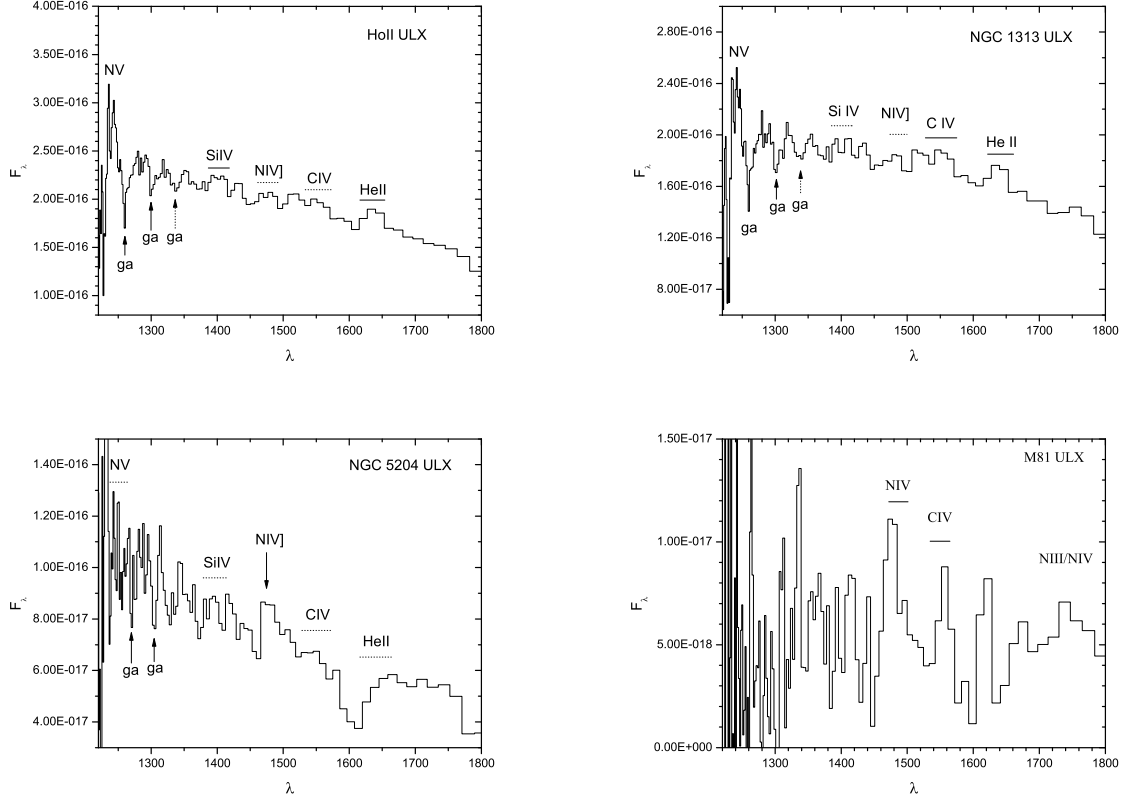


Fig. 1.— The HST/ACS prism spectra for the four ULXs in (a) Ho II, (b) NGC1313, (c) NGC5204, and (d) NGC3031. Labeled are the three galactic absorption lines (Si II  $\lambda$ 1260.4, O I  $\lambda$ 1302.2, and C II  $\lambda$ 1334.5), doublet lines NV  $\lambda$ 1238.8, 1242.8, Si IV  $\lambda$ 1393.8, 1402.8, C IV  $\lambda$ 1548.2, 1550.8, semi-forbidden line N IV  $\lambda$ 1486.5, and He II  $\lambda$ 1640.4. Dotted lines under the symbol for the ion shows where the ion should lie but that there is not a likely detection. Galactic absorption lines are noted with the symbol ga. The range in the flux density is similar, a factor of five, except for (d).

$\lambda 1260.4$  line, which is not symmetric on the red side in the sense that it is consistent with an additional absorption feature that is typical of this stellar line. The next stellar line, at Si III  $\lambda 1298.9$ , lies to the blue of the Galactic O I  $\lambda 1302.2$  line. The minimum of the absorption feature corresponds to the Si III line rather than the O I line. The next stellar line, O IV  $\lambda 1338.61$ , is also close to a Galactic absorption line, C II  $\lambda 1334.5$ , with the spectral minimum lying between the two features.

We can infer the velocity width of the N V  $\lambda 1240$  emission lines by comparing it to the Si II  $\lambda 1260.4$  line, which has a FWHM of about  $3.6\text{\AA}$ , consistent with the instrumental resolution. This is narrower than the width of the N V  $\lambda 1240$  doublet, where the blue side is poorly defined due to the rapidly decreasing sensitivity. When we use the red side of this emission line to define the line width, we obtain a FWHM of  $6\text{\AA}$ . The inferred intrinsic FWHM is  $5\text{\AA}$ , after compensating for instrumental resolution, so if the FWHM is characteristic of the outflow or rotational velocity, it would be about  $600\text{ km s}^{-1}$ .

NGC 1313: The spectrum is similar to that of Holmberg II, showing the same Galactic absorption features, along with the N V and He II emission features. There is likely broad emission corresponding to C IV  $\lambda 1550$ , but other features are not statistically significant. There is a broadened red wing to the Si II  $\lambda 1260.4$  line, which could be due to the stellar Si II  $\lambda 1264.7$  line, but better data are needed to confirm this. There are no suggestions of the other stellar features. The line width of the N V  $\lambda 1240$  emission is the same, to within statistical uncertainties, with the one seen in Holmberg II.

NGC 5204: The continuum is a few times weaker than Ho II, so some lines visible in Ho II would not be expected to be significant here. The strongest Galactic absorption line, Si II  $\lambda 1260.4$ , is not detected. The Galactic O I  $\lambda 1302.2$  may have been detected, although the line center is at  $1304.2\text{\AA}$ . This shift could be due to absorption within the disk of NGC 5204. In emission, the N V  $\lambda 1240$  feature is not detected, nor is He II  $\lambda 1640$  or C IV  $\lambda 1550$ . There is an apparent emission feature with a peak at  $1478.3\text{\AA}$ , so it is possible that this is the WN feature N IV  $\lambda 1486$ , if there is a calibration wavelength offset. A local minimum at  $1610\text{\AA}$  does not correspond to any known feature.

Messier 81: The UV fluxes are about a factor of 20 lower than for Ho II, so only emission lines would be evident, as a continuum would be too weak to reliably detect. The strongest feature has a central wavelength of about  $1477\text{\AA}$ , as seen in NGC 5204. This may be the WN feature N IV  $\lambda 1486$ , with a wavelength offset. There may be emission from the C IV  $\lambda 1550$ , which is close to the correct wavelength ( $1556\text{\AA}$ ), and the effect of a P–Cygni profile, if present, is to shift the line to longer wavelength. There is a weak peak at the location of Si IV  $\lambda 1400$ . There is no detection of He II  $\lambda 1640$  emission. Two features at  $1310\text{\AA}$  and  $1337\text{\AA}$  are unidentified and are narrower than the instrumental resolution, so unlikely to be real.

#### 4. Interpretation of the Spectra

In order to understand the features and nature of the spectra, we took a variety of UV spectra that represent different types of objects and convolved them with the varying spectral resolution of the prism. A brief discussion of each class, with examples are given below and we have tried to retain the same scale as for the ULX sources, which is a factor of five in the vertical scale and for a wavelength range of 1220-1800Å.

**OB Stars:** Most of the OB stars examined are dominated by a stellar continuum with a few absorption features due to the intervening interstellar medium (Fig. 2a) as well as some weak stellar absorption line features, such as Si III  $\lambda$  1298.9, Si III  $\lambda$  1417.2, or He II  $\lambda$  1640.4 (Prinja et al. 1990). A very hot star, such as a planetary nebula central star (Fig. 2b) has nearly a Rayleigh-Jeans power-law shape over this wavelength range, punctuated by absorbing features in the ISM. Some O stars have stellar winds, displaying P–Cygni profiles, signatures that we see strongly in the Wolf-Rayet stars and the high mass X-ray binaries.

**Wolf-Rayet Stars:** There is a very wide range of spectral behavior for the various classes of WR stars, but line emission is a common property, although the line strengths can vary dramatically. The WN4 (Fig. 2c) star shows a typical spectrum, with a strong He II line, followed by lines of N V, Fe V/O V, C IV, and N III/N IV. The P–Cygni profiles are washed out at the resolution of the PR130L and the peak of the line appears to shift from its normal value. At prism resolution, the P–Cygni profile for C IV  $\lambda$  1550 results in an absorption dip surrounded by local peaks, which is common for hot wind outflows. For a WN8 star (Fig. 2b), which has a lower degree of ionization, the He II line is weaker, and at the resolution of the prism, it is not significant. Lines of NIII and NIV are visible and there is a dip at the location of C IV  $\lambda$  1550 but it might not be considered significant. There is no NV  $\lambda$  1240 emission and the blue part of the spectrum is suppressed, either due to extinction or to a lower temperature for the star. Toward earlier WN type (higher ionization), the He II  $\lambda$  1640 line becomes dominant and the N V  $\lambda$  1240 line is present. The WC stars have a much stronger (and often dominant) C IV  $\lambda$  1550 line and weak nitrogen lines.

**High Mass X-Ray Binaries:** In these cases, the compact object is a black hole or neutron star and the star is of early type with mass loss that includes and can be dominated by a stellar wind. The object 4U1700-37 (Fig. 3a) is a good example where the compact object has a mass of  $2.4 M_{\odot}$ , and it is not clear if this is a NS or BH. The massive star is type O6.5Iaf, with a mass of  $58 M_{\odot}$  and an orbital period 3.4 days. It has strong P-Cygni emission lines of NV, Si IV, and CIV, with a weak He II  $\lambda$  1640 line (Fig. 3a). At the resolution of the PR130L, only an absorption feature survives near 1550Å, the He II line is not significant, but the Si IV and NV emission is present, with the P-Cygni profile still visible for Si IV. Another example of this class, Cyg X-1 (Fig. 3b) does not show P-Cygni profiles, but does

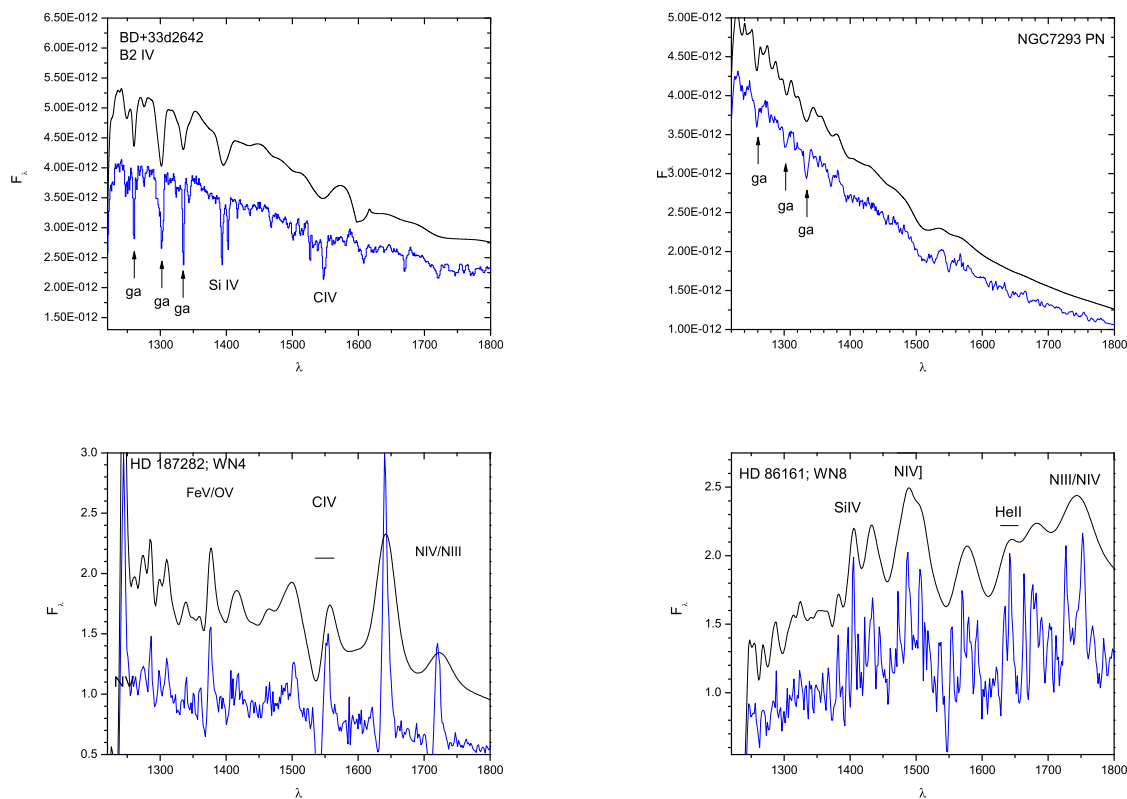


Fig. 2.— The IUE spectra for (a) a hot B2IV star BD+33d2642, (b) a planetary nebula central star in NGC7293, (c) a WN4 star HD 187282, and (d) a WN8 star HD 86161. The smoothed curves are obtained by convolving the IUE spectrum with the varying spectral resolution of the HST/ACS prism. The range in flux density is a factor of five for all spectra except for (c), where it is a factor of six.



show absorption features corresponding to Si IV and C IV.

Intermediate Mass X-Ray Binaries: These systems have a black hole or neutron star with a star of 2-6  $M_{\odot}$  in orbit. Examples are LMX X-3 (black hole plus 5.9  $M_{\odot}$  star) or Her X-1 (HZ Her; a neutron star plus a 2.3  $M_{\odot}$  star), and in the latter case, the strongest emission feature is NV  $\lambda$  1240, followed by C IV  $\lambda$  1550 and He II  $\lambda$  1640, which is a small feature at the resolution of the prism (Fig. 3c). A N IV]  $\lambda$  1486Å line is visible in LMC X-3, along with C IV  $\lambda$  1550, but the NV line is the strongest feature (Fig. 3d).

Low Mass X-Ray Binaries: Typically, these have a neutron star with a companion star of about  $1M_{\odot}$ , with Sco X-1 or Cen X-4 being examples (Fig. Cen X-4). The strongest features are usually NV  $\lambda$  1240, Si IV  $\lambda$  1400, C IV  $\lambda$  1550, and He II  $\lambda$  1640, all of which are visible at the prism resolution with the exception of the He II line, which can appear weak. In Sco X-1, the C IV line is the strongest FUV feature (Fig. 4c).

White Dwarf Systems: We mention these for completeness, as they are certainly not responsible for the ULX systems but have relevant UV spectra. The cataclysmic binary SS Cyg has a white dwarf of mass 0.40  $M_{\odot}$  and a dwarf star of 0.6  $M_{\odot}$ , and its UV spectrum shows a very strong line of CIV  $\lambda$  1550Å, a somewhat weaker Si IV  $\lambda$  1400Å feature, and weaker lines NV  $\lambda$  1240Å, He II  $\lambda$  1640Å, and two lower ionization lines of OI and C II (Fig. SSCyg). Supersoft sources, which we assume have a white dwarf as the compact object, such as RXJ 0513.9-6951, have strong lines of He II 1640Å and N V 1240Å (Fig 4d).

#### 4.1. Comparison to the ULX Prism Spectra

In comparing these spectra to the four ULX systems, we begin with Ho II ULX and NGC 1313 ULX, which are quite similar to each other (Fig. 1a-b). They both show the N V  $\lambda$  1240 feature as their strongest emission line, found in most classes of mass-transfer binaries. These spectra indicate that the two ULX candidates are not single O/B stars, thus confirming the identification of the optical counterpart. There is no strong absorption feature at the location of the Si IV  $\lambda$  1400 or C IV  $\lambda$  1550 doublets, which are characteristic of HIMXBs and early-type WR stars. This would indicate that these two ULX systems are not HIMXBs in which the mass transfer is dominated by winds. The closest match of these two ULX spectra is with intermediate mass XRBs, although the match is not perfect. In HZ Her, the equivalent width of the N V  $\lambda$  1240 line is nearly four times larger than the ULXs in Ho II or NGC 1313, with a relative difference in the same sense for the C IV  $\lambda$  1550 line (Table 1). In contrast, the ULXs have relatively stronger He II  $\lambda$  1640 lines than in HZ Her, but the difference is only 40%. These relative equivalent width differences are

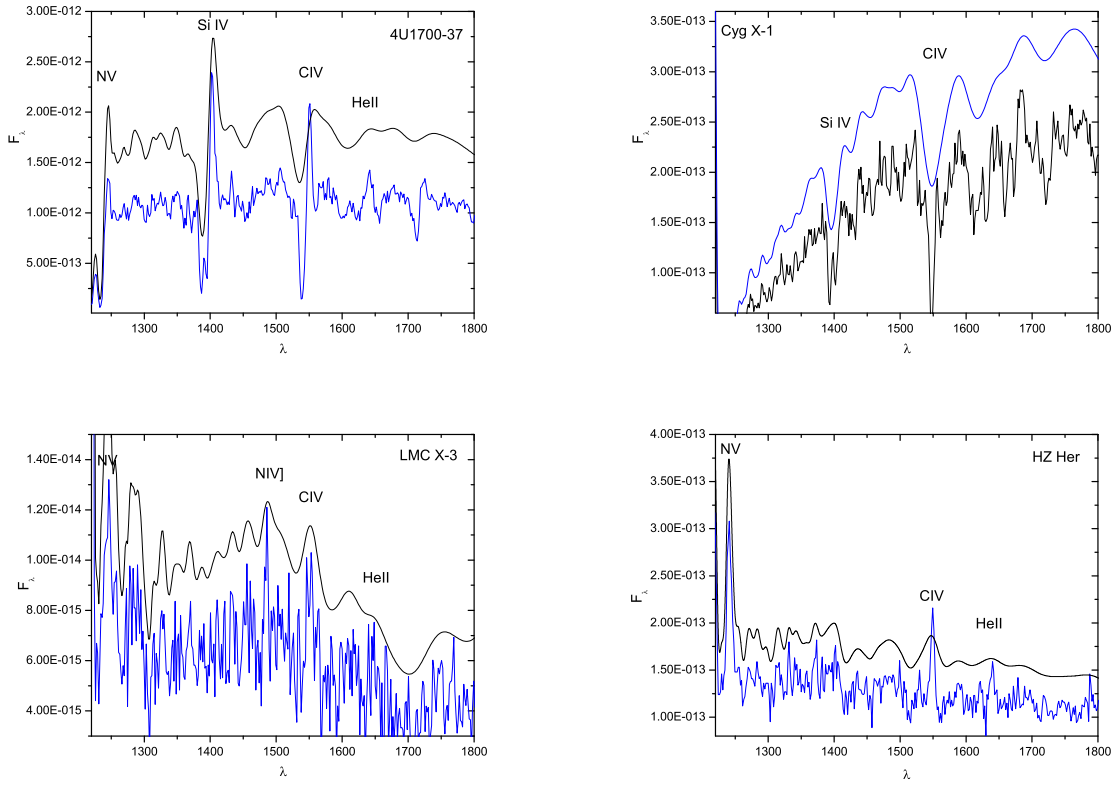


Fig. 3.— The IUE spectra for (a) a HMXB 4U1700-37, (b) a HMXB Cyg X-1, (c) an IMXB LMC X-3, and (d) an IMXB Her X-1. The smoothed curves are obtained by convolving the IUE spectrum with the varying spectral resolution of the HST/ACS prism.

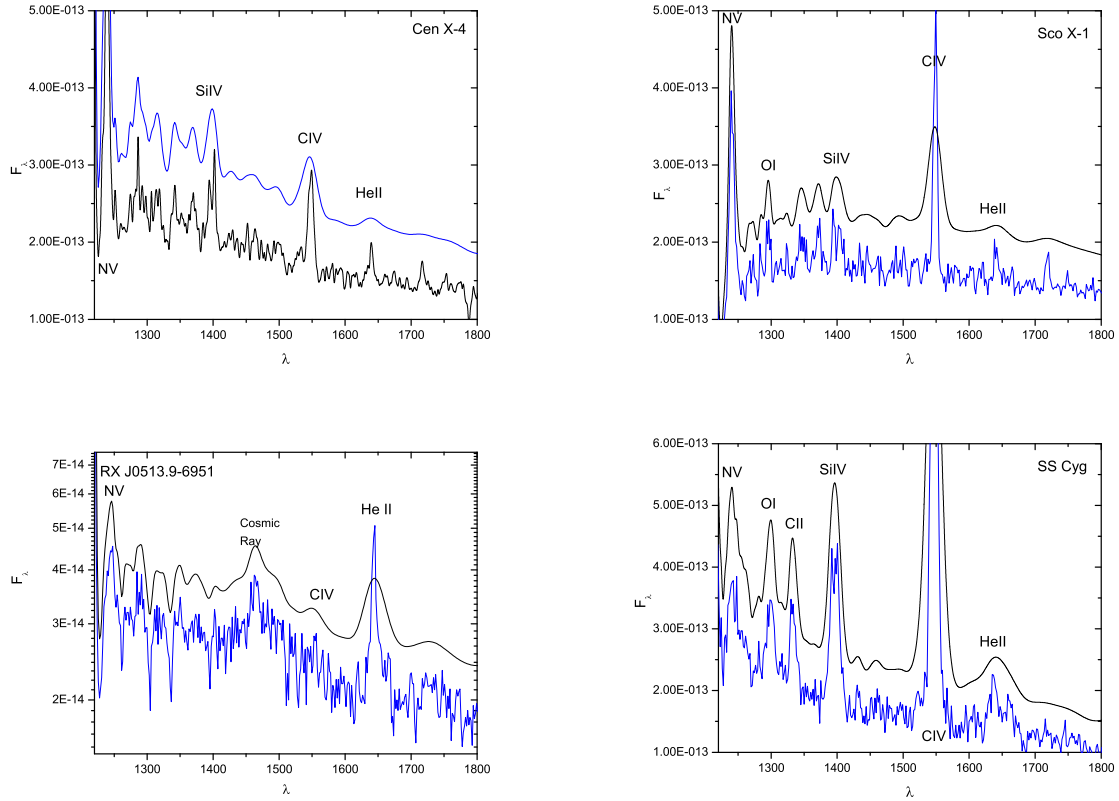


Fig. 4.— The IUE spectra for (a) a LMXB Cen X-1, (b) a LMXB Sco X-1, (c) a supersoft source RX J0513.9-6951, and (d) a cataclysmic variable SS Cyg. The smoothed curves are obtained by convolving the IUE spectrum with the varying spectral resolution of the HST/ACS prism.

also true for a comparison to the LMXB Cen X-4, with the similarity to HZ Her probably due to a common structure to the accretion disk, although the C IV  $\lambda$  1550 line is stronger in Cen X-4. The differences between the ULX spectra and that of the HZ Her may be due to a lower metallicity in the donor star for the ULX systems, it could be due to greater continuum dilution by the ULX donor stars, or it could indicate a more significant difference in the structure of the accretion disk.

The ULX in NGC 5204 is the only ULX source with a good-quality STIS low resolution far UV spectrum, previously reported by Liu et al. (2004; Fig. 5). The STIS G140L spectrum is of higher S/N than that from the prism, and we compare the two by convolving the STIS spectrum to the resolution of the prism. The N V  $\lambda$  1240 line is present at about the same EW as the previous two ULX systems (note that the other ULX sources are more than twice as bright and have higher S/N). A few other weak emission sources are known from the STIS spectrum (marked in figure), but emission from C IV  $\lambda$  1550 was not detected while the He II  $\lambda$  1640 is formally present at about the 4-5  $\sigma$  level. The convolved STIS spectrum is consistent with the prism spectrum, showing the O I/SiII emission feature, preceded by absorption. The NGC 5204 ULX system is similar to the ULX systems in NGC 1313 and Ho II. With the STIS spectrum, stellar photospheric lines are detected, which allows for a separation of disk and secondary, which is type B0 Ib (Liu et al. 2004), or about 25  $M_{\odot}$  (Schmidt-Kaler 1982). This secondary is more massive and more luminous than the counterpart in HZ Her. Consequently, it would be expected that the stellar continuum is relatively more significant than the lines, diminishing their equivalent widths. Another possibly important feature is the presence of the N IV]  $\lambda$  1486 line, seen tentatively in each ULX prism spectrum but detected above the 5 $\sigma$  level in the STIS spectrum of NGC 5204. This semi-forbidden line is not detectable in a stellar photosphere because the density is above the critical density. It is not predicted in flat accretion disks with atmospheres (Raymond 1993), nor is it detected in LMXB or CV systems, but it is detected in some IMXB systems, such as LMX X-3. For this line to occur, there must be an adequate emission measure of gas that is strongly excited, which can occur in outflows, such as in Wolf-Rayet stars, but this is not the only possibility.

The flux density of the ULX in M81 is about 30 times lower than for the ULXs in NGC 1313 or Ho II, so the quality of the features is poor (Fig. 1d). The N V  $\lambda$ 1240 emission line is not detected given the low S/N at the blue end, although there is an indication of emission near this wavelength. Three possible emission features in the spectrum as labeled in Fig. 1d would appear to be most similar to the late-type Wolf-Rayet star, HD86161 (Fig. 2d), although better quality data is needed to examine this possibility.

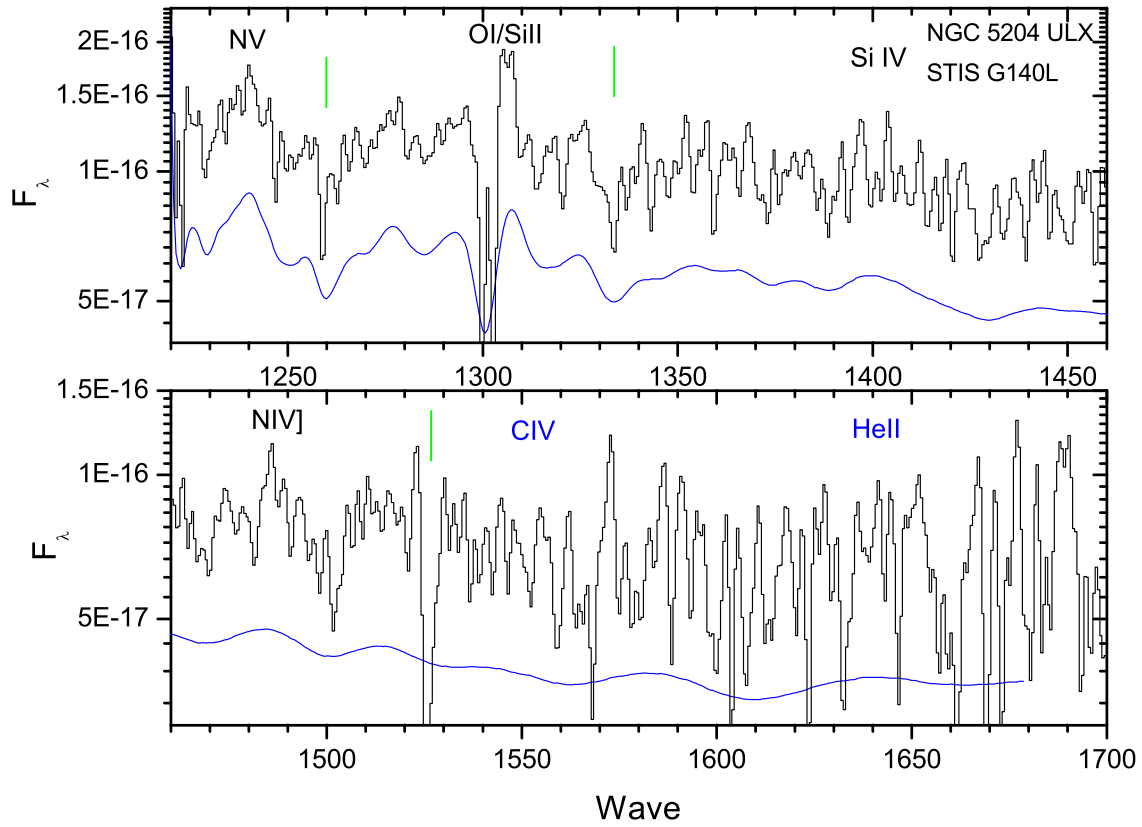


Fig. 5.— The HST/STIS FUV spectrum for the ULX in NGC5204. The smoothed curve is obtained by convolving the IUE spectrum with the varying spectral resolution of the HST/ACS prism.

## 4.2. Color-Color Plots

In addition to using the spectral features of ULXs and comparison sources, we can also use the shape of the continuum. The reason for using this is that there are different expectations for the shape of the continuum from a multi-temperature disk and from a hot star. Thus, it may be possible to distinguish between a continuum dominated by an accretion disk and a continuum dominated by hot stars.

There are a few challenges facing this approach, such as choosing the location of the continuum points and compensating for extinction along the line of sight. For the continuum points, we chose locations that are not dominated by emission lines yet provide the best leverage for a two-color analysis: 1300Å; 1500Å; and 1800Å. The second issue is compensating for the extinction, but the reddening vector can be determined from the extinction law of Cardelli et al. (1992). The ULXs are known to generally occur in regions of extinction where the intervening column is typically  $1\text{-}5 \times 10^{21} \text{ cm}^{-2}$ , although the metallicity is often sub-solar. Extinction usually affects hot stars, which occur near their dust-rich birth sites. Also, many of the XRBs lie in the disk of the Milky Way, where extinction can be considerable.

In our UV color-color analysis, we also show the color expected from a standard multi-temperature disk, where  $F_\nu \propto \nu^{1/3}$ , as well as the Rayleigh-Jeans limit ( $F_\nu \propto \nu^2$ ) to the blackbody curve. A very hot star would approach this Rayleigh-Jeans limit, but as the star becomes progressively cooler, it approaches the multi-temperature disk line for a blackbody temperature of about  $2.5 \times 10^4 \text{ K}$  in the chosen color bands as shown in Figure 6. The XRBs of various types scatter around the multi-temperature disk line. The heavily reddened Cygnus X-1 lies on this relationship, indicating that the choice of the reddening law leads to sensible results. The stars, which are mostly hot, are distributed from the Rayleigh-Jeans line to the multi-temperature disk line. The Wolf-Rayet stars indicate significant extinction, as would be expected for stars with a large amount of mass loss and embedded in star forming regions, while many of the other hot stars were chosen because of their more modest absorption, and they lie lower in the diagram. The ULX sources lie between the multi-temperature disk model and the Rayleigh-Jeans model, somewhat more to the Rayleigh-Jeans side of the XRBs. This is consistent with a model where the ULX sources are a combination of a stellar continuum and an accretion disk source. From the spectral analysis, we concluded that the ULX in NGC 5204 has a higher ratio of stellar continuum and that the ULXs in NGC 1313 and Ho II have relatively more accretion disk emission. Their location on the color-color plot is consistent with that interpretation, as those latter two ULXs have colors closer to the multi-temperature disk line. We view this approach as a useful consistency check for our interpretation of the ULX spectra.

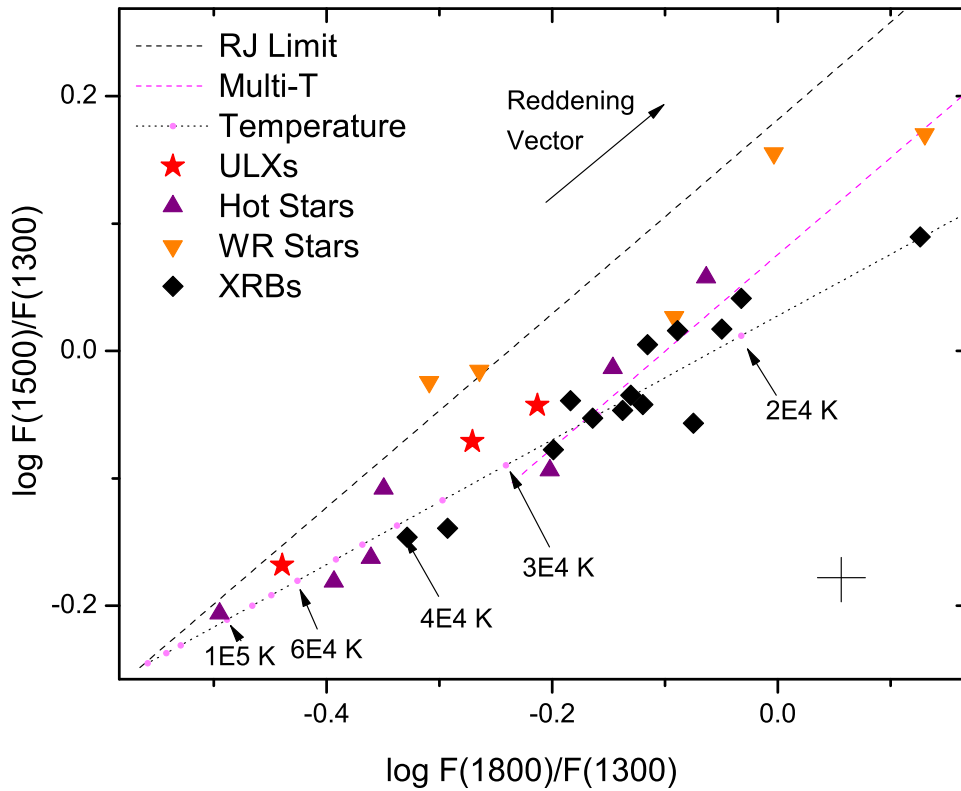


Fig. 6.— Color-color diagram for the four ULXs and other known objects. Overplotted curves include the reddening vector, the standard multi-temperature disk and the Rayleigh-Jeans limit with varying extinction, and the black body models with different temperatures. The S/N of the ULX in M81 was too poor to provide useful color data, so that object is not included.

## 5. Discussion

One of the primary goals of this work was to determine whether the optical counterparts, identified by finding an object within an error circle, was indeed the donor star in the ULX binary system. For the ULX in NGC 5204, this was already established from a STIS UV spectrum (Liu et al. 2004), which showed the N V  $\lambda$  1240 emission feature, a feature predicted to be strong for accretion disk systems (Raymond 1993). For the ULX optical counterparts in NGC 1313 and Ho II, there were significantly stronger UV emission line features, which may be due to a larger contribution from the accretion disk relative to the star. For the ULX in M81, this line is not detected due to the low S/N at the blue end, but there is an indication of emission near this line.

The stellar mass can be estimated from the magnitude and color with the help of the high resolution UV spectrum. In the case of NGC5204, the high resolution STIS spectrum was available, which showed stellar photospheric lines and allowed for a separation of the disk and a B0Ib secondary of about  $25M_{\odot}$  (Liu et al. 2004). No such mass estimates are made for the ULXs in Ho II and NGC1313 because there is a degeneracy with spectral type due to the unknown fraction of emission coming from the accretion disk. This degeneracy can be removed with a higher resolution UV spectrum, which is possible with current instruments on HST.

The secondary mass for the ULX in Ho II has been estimated in previous works with the help of emission lines in other bands. Strong He II  $\lambda$ 4686 emission line was detected in the surrounding nebula produced by X-ray photoionization, and the secondary is estimated to be in the range of B3Ib to O4V based on the optical data (Kaaret et al. 2004). With Spitzer, Berghea et al. (2010) detected the [OIV]  $25.89 \mu\text{m}$  line, and estimated the secondary to be a B2Ib supergiant based on the overall spectral energy distribution from X-ray to UV to infrared. Such a secondary is about  $20M_{\odot}$ , similar to the secondary in NGC 5204.

For the ULX in NGC1313, the secondary mass is estimated from  $\sim 8.5M_{\odot}$  (Liu et al. 2007) to  $\sim 20M_{\odot}$  (Mucciarelli et al. 2005) based on the optical magnitudes and different separation of the secondary and disk contribution. Recently, Liu et al. (2012) estimated the secondary to be a  $\sim 8M_{\odot}$  evolved star based on the dynamical constraints by combining the HST light curves, including the orbital period of  $\sim 6$  days (Liu et al. 2009), and the radial velocity amplitude measured from the He II  $\lambda$ 4686 emission line from the disk (Roberts et al. 2011). In this model, the emission is dominated by the accretion disk; this is consistent with the stronger N V  $\lambda$  1240 emission line as compared to the case of NGC 5204.

There is a similarity in the nature of the secondary for the ULX counterpart in NGC 1313, Ho II, and NGC 5204 in that they are blue evolved stars of about 8–20  $M_{\odot}$ . By



mass, this might suggest that they are high mass X-ray binaries, in which mass transfer is often through stellar winds. However, these systems do not show in the UV P-Cygni like absorption features that accompany HIMXBs. Rather, these are similar to the intermediate mass binaries, where the mass transfer is through Roche Lobe overflow. If this type of configuration is common in ULXs, it could indicate the binary properties necessary for the ULX phenomenon to occur.

The authors gratefully acknowledge valuable commentary and assistance from a variety of people, including Jon Miller, Jimmy Irwin, Sally Oey, Charles Cowley, Mark Reynolds, and Ed Cackett. We gratefully acknowledge financial support for this work from NASA. Some of the data presented in this paper were obtained from the Mikulski Archive for Space Telescopes (MAST). STScI is operated by the Association of Universities for Research in Astronomy, Inc., under NASA contract NAS5-26555. Support for MAST for non-HST data is provided by the NASA Office of Space Science via grant NNX09AF08G and by other grants and contracts.

## REFERENCES

- Begelman, M.C., 2002, *ApJ*, 568, L97
- Berghea, C. T.; Dudik, R. P.; Weaver, K. A. & Kallman, T. R., 2010, *ApJ*, 708, 354
- Cardelli, J; Sembach, K. & Mathis, J., 1992, *AJ*, 104, 1916
- Colbert, E. J. M. and Mushotzky, R. F. 1999, *ApJ*, 519, 89
- King, A. R., Davies, M. B., Ward, M. J., Fabbiano, G. and Elvis, M. 2001, *ApJ*, 552, L109
- Kümmel, M., Walsh, J.R., Pirzkal, N. et al. 2009, *PASP*, 121, 59
- Liu, J. & Bregman, J., 2012, *ApJS*, submitted
- Liu, J., Bregman, J., and Seitzer, P., 2002, *ApJL*, 580, 31
- Liu, J., Bregman, J., and Seitzer, P., 2004, *ApJ*, 602, 249
- Liu, J.; Bregman, J.; Miller, J. & Kaaret, P., 2007, *ApJ*, 661, 165
- Liu J., Bregman J., & McClintock, J., 2009, *ApJL*, 679, 37
- Liu, J., Orosz, J., & Bregman, J., *ApJ*, 2012, 745, 89

- Mucciarelli, P.,Zampieri, L., et al. 2005, ApJ, 633, L101
- Niedzielski, A. & Rochowicz, K., 1994, A&AS, 108, 669
- Prinja, R.K., 1990, MNRAS, 246, 392
- Raymond, J. 1993, ApJ, 412, 267
- Roberts, T. P., Gladstone, J.C., Goulding, A.D., et al. 2011, AN, 332, 398
- Schmidt-Kaler, Th., 1982, *Landolt-Bornstein: Numerical Data and Functional Relationships in Science and Technology*, eds. Schaifers, K. and Voigt, H.H., VI/2b, P.15-31

---

This preprint was prepared with the AAS L<sup>A</sup>T<sub>E</sub>X macros v5.2.

Table 1. Emission Line Equivalent Widths

Binary Name	Type	NV	CIV	HeII	F(NV)	F(He II)	F <sub>x</sub>
Ho II	ULX	$2.7 \pm 0.3$	$< 2$	$2.4 \pm 0.4$	6.1E-16 (6)	4.2E-16 (5)	1.2E-11
NGC 1313	ULX	$2.7 \pm 0.3$	$< 2$	$2.4 \pm 0.4$	5.2E-16 (6)	3.8E-16 (5)	5E-12
NGC 5204	ULX	$2.9 \pm 0.4$	$< 2$	$2.0 \pm 0.4$	2.8E-16 (5)	1.2E-16 (3)	2E-12
HZ Her	IMXB	$10. \pm 1.$	$3.2 \pm 0.3$	$1.7 \pm 0.3$			
Cen X-4	LMXB	$11. \pm 1.$	$7.0 \pm 0.7$	$1.5 \pm 0.2$			